Integrative Biology

Accepted Manuscript

ROYAL SOCIETY OF CHEMISTRY

www.rsc.org/ibiology

Insight, innovation, integration

This work brings new insights on compartmentalized microfluidic devices herein showed, for the first time, to be an innovative tool to study sensory neurons and non-neuronal cells interactions, surpassing the limitations of the currently available systems. We explored this platform to perform explants cultures of sensory neurons and osteoblasts. Moreover we enriched the non-neuronal cells/axonal microenvironment for 2D/3D cocultures as a step forward to extracellular matrix interaction studies. We also improved the system's readout by developing a computational application for quantify axonal growth within non-neuronal cells in these platforms.
Overall we developed a tool for studies of the peripheral tissues innervation in physiological/pathological conditions which can be integrated in different fields such as drug delivery or tissue engineering approaches.

Cite this: DOI: 10.1039/c0xx00000x

www.rsc.org/xxxxxx

PAPER

Sensory neurons and osteoblasts: close partners in a microfluidic platform

Estrela Neto [a,b], Cecília Juliana Alves [a], Daniela Monteiro Sousa [a], Inês Soares Alencastre [a], Ana Henriques Lourenço [a], Luís Leitão [c], Hyun Ryul Ryu [d], Noo Li Jeon [d,e], Rui Fernandes [c], Paulo Aguiar [f], Ramiro Daniel Almeida [g] and Meriem Lamghari* [a,h]

Received (in XXX, XXX) Xth XXXXXXXXX 20XX, Accepted Xth XXXXXXXXX 20XX
DOI: 10.1039/b000000x

Innervation has proven to be critical in bone homeostasis/regeneration due to the effect of soluble factors, produced by nerve fibers, associated with changes in bone cells activity. Thus, in this study, we have established and characterized a coculture system comprising sensory neurons and osteoblasts to mimic the *in vivo* scenario where nerve fibers can be found in bone microenvironment. Embryonic or adult primary dorsal root ganglion (DRG) and MC3T3-E1 osteoblastic cells were cocultured in compartmentalized microfluidic platforms and morphological and functional tests were performed. The time of adhesion and readout of axonal outgrowth were improved by the alignment of DRG, with the axis of microgrooves, which showed to be a crucial step for the designed experiments. Cocultures of entire DRG from adult origin with osteoblasts were performed, showing extended DRG projections towards the axonal compartment, reaching osteoblastic cells. Immunocytochemistry showed that the neurites present within osteoblastic compartment were immunoreactive to synapsin and calcitonin gene-related peptide suggesting the presence of specialized structures involved in this crosstalk. These evidences were further confirmed by electron microscopy where varicosities were detected as well as electron dense structures in neurites membrane. Aiming to mimic the properties of tissue extracellular matrices, MC3T3-E1 cells were seeded in the axonal side upon laminin, collagen or within 3D functionalized alginate matrices and axonal outgrowth was clearly observed. In order to analyze and quantify data with reproducible image analysis, a semi-automated algorithm was also developed. The collagen and laminin substrates displayed a higher amount of axons reaching the axonal side. Overall, the established method revealed to be a suitable tool to study the interaction between peripheral nervous system and bone cells in different contexts mimicking the *in vivo* scenario.

Introduction

Bone remodeling is a reaction to internal/external stimuli and it is essential to maintain ion homeostasis and to replace damaged bone. It has been conventionally linked to hormones and mechanical loading[1, 2, 3] however, in the last decade, several studies provided evidence that bone homeostasis is also under the influence of central and peripheral neural control (reviewed in Franquinho *et al.*[4]). Sensory and sympathetic fibers have been detected in bone marrow and mineralized bone.[5, 6, 7] Furthermore, in a regeneration scenario, an intense nerve regeneration was observed to occur early during fracture healing[8] and this process was impaired in bone deinnervated animals,[9, 10] highlighting the importance of innervation in bone regeneration. Nevertheless, the intricate mechanisms underlying the communication between peripheral nervous system and bone cells remain to be revealed and further studies in this field are required.

In order to study the interactions between different biological systems in an accurate environment, coculture systems are widely used.

The majority of the existent studies concerning neurons and osteoblasts lineage were performed with cell-cell contact cultures that do not mimic the *in vivo* scenario. For instance, coculture experiments have been performed using osteoblasts and Schwann cells,[11, 12] osteoblasts and sensory neurons,[13, 14] osteocytes and dissociated dorsal root ganglion (DRG)[15] and bone marrow stromal cells and DRG.[16] However, the methods used so far are not consensual since DRG houses the cell bodies of the afferent fibers from the periphery.[17] Therefore, novel approaches are needed to establish an *in vivo*-like microenvironment, where only the projected neurons will contact with the bone cells.

In a wide range of coculture techniques, microfluidic devices are becoming frequently used.[18] Miniaturized components, reduced sample volumes and reaction times, higher data quality and reliable parameter control represent advantageous strategies to study the cell behavior at a small scale and in a controlled microenvironment.[19]

Microfluidic compartmentalized devices were mainly used for neuroscience research to examine a wide range of neural

functions, from axonal transport to injury and regeneration, due to their unique ability to allow high-resolution live imaging. The compartmentalization of these devices relies on microgrooves contained within a solid barrier through which axons and dendrites are able to extend, but not their cell bodies.[20, 21] These devices have strong potential for applications at the interface of neuroscience, developmental cell biology, advanced biomaterials and microfluidic technology.[21] Indeed, an increasing number of studies are being published,[22, 23] reporting novel discoveries in cell biology such as the study of endothelial and mesenchymal stem cells' migration,[24] epithelial cells and fibroblasts interactions,[25] and in mesenchymal stem cells and neuronal cells transdifferentiation studies.[26]

Given the importance of innervation in bone microenvironment and the lack of adequate tools to study the interaction between peripheral nervous system and bone cells, in this study we propose to explore and validate a compartmentalized microfluidic device for the coculture of neuronal and non-neuronal cells, namely osteoblasts. In the scope of tissue engineering, the extracellular matrix of the bone microenvironment was simulated using different substrates for the osteoblasts. Additionally, we have also developed a computational application of a mathematical algorithm, which enabled the automatic quantification of neurite outgrowth within microfluidic context.

Results

Neurite outgrowth within osteoblastic compartment

Microfluidic devices were explored and optimized as the coculture platform to obtain a system that could gather the conditions to mimic the *in vivo* bone microenvironment by preserving the ability of the nerve fibers to reach and communicate with osteoblasts.

Prior to assemble the coculture system both sensory neurons/entire DRG and MC3T3-E1 cells were cultured alone in the compartmentalized microfluidic device (Fig. 1A). In the somal side, dissociated embryonic sensory neurons and entire DRG from adult origin were cultured. Immunocytochemistry against βIII tubulin (neuronal marker) was assessed to observe the development of DRG culture in microfluidic device. As shown in Fig. 1B and 1C, dissociated embryonic neurons and entire DRG from adult mice were able to adhere and develop a dense and uniform network of axons.

In the axonal side, osteoblasts were cultured at different cell densities (1.5 x 10^4, 1.5 x 10^5 and 3 x 10^5 cells/cm^2) to identify the cell number that allows the maintenance of cell morphology, viability and also cell confluence as well as to avoid cells crossing the microgrooves to the somal side. While no cell confluence was observed for the lower density tested (1.5 x 10^4 cells/cm^2), at higher cell density (3x10^5 cells/cm^2) cells have crossed the microgrooves towards the somal side (Fig. 1D). The cell number of MC3T3-E1 cells used to conduct the coculture was 1.5 x 10^5 cells/cm^2 (corresponding to a total number of 1.5 × 10^4 cells per microdevice). The metabolic activity was assessed by MTT assay to ensure that spatial restrains were not affecting cell behavior. An increase of the metabolic activity of MC3T3-E1 cells, seeded in the axonal side of the microfluidic device, was observed (Fig. 1E) when compared to the control (monoculture in a 96-well plate).

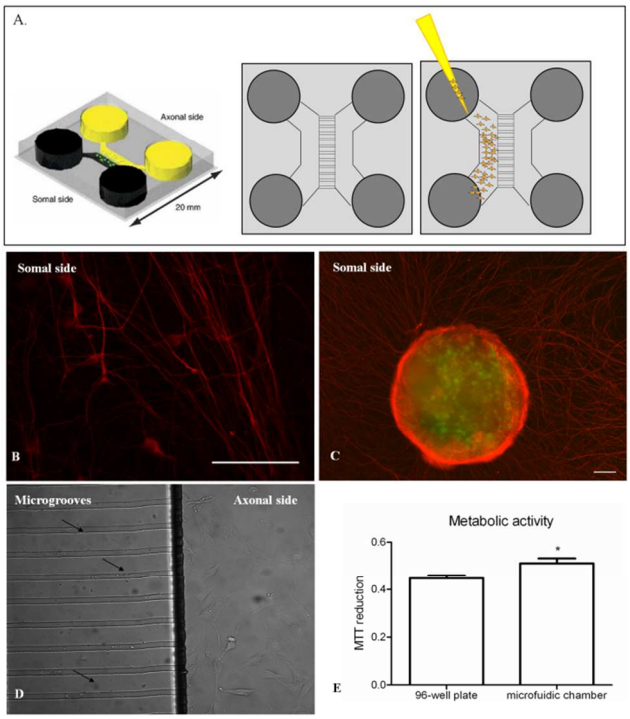

Fig.1 A. Seeding of dissociated cells. Schematic representation of microfluidic platforms and process of cell seeding. Dissociated cells were suspended in media and seeded in somal side of the device. Adapted by permission from Macmillan Publishers Lta: Nature Methods,[20] copyright 2005. B. Dissociated embryonic sensory neurons cultured in somal side. Neurons were stained against βIII tubulin (red). C. Representative image of an entire adult DRG cultured in the microfluidic chamber for explants. The entire DRG adhered to the coverslip and developed an uniform neurite network. Neurons were stained against βIII tubulin (red) and actin with Alexa-488 Phalloidin (green). Scale bar 100 μm D. MC3T3-E1 cells seeded on axonal side of the microfluidic chamber (3.0 x 10^5 cells/cm^2) at day 3 of culture. MC3T3-E1 cells crossing the microgrooves towards the somal side (black arrows). E. Metabolic activity of MC3T3-E1 cells in the microfluidic chambers measured after three days of culture using MTT assay. Data were expressed as mean ± S.E.M. Statistical differences were considered when *p<0.05.

For the coculture experiments, dissociated embryonic sensory neurons or entire DRG from adult origin and MC3T3-E1 cells were seeded on the somal and axonal side, respectively. Cocultures were monitored for three days. In the somal side the embryonic sensory neurons or the adult entire DRG (stained against βIII tubulin) showed to be able to grow neurites towards the axonal side throughout microgrooves (Fig. 2). MC3T3-E1 cells, seeded in the axonal side, were confluent and exhibited a characteristic polygonal shape, similar to controls in monocultures (Fig. 2). Importantly, axons were detected within osteobalstic compartment where no axonal degeneration was observed.

The cocultures were successfully performed with both embryonic sensory neurons and entire DRG from adult origin. In the axonal side, it was possible to observe neurite outgrowth independent on the sensory neurons source used.

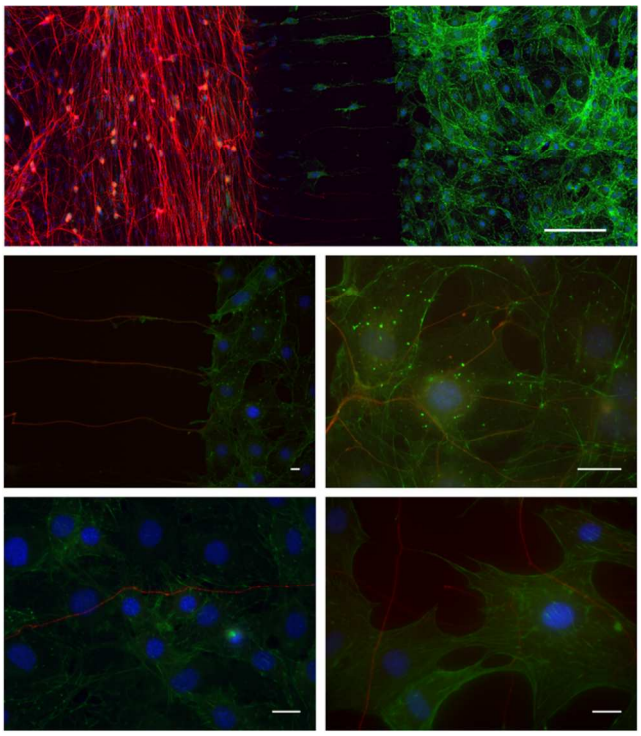

Fig.2. Representative images of three days coculture system regarding MC3T3-E1 cells plus dissociated embryonic DRG (low magnification on top and higher magnifications on center), and MC3T3-E1 cells plus entire DRG (bottom). MC3T3-E1 cells were stained in green for F-actin, neurons in red for βIII tubulin and nuclei in blue with DAPI. Scale bar 500 μm, upper image and 20 μm center and bottom.

Alignment of DRG in somal side

Cocultures were successfully performed, however variability among the tested coculture systems was observed, namely regarding the axonal network within the osteoblastic compartment.

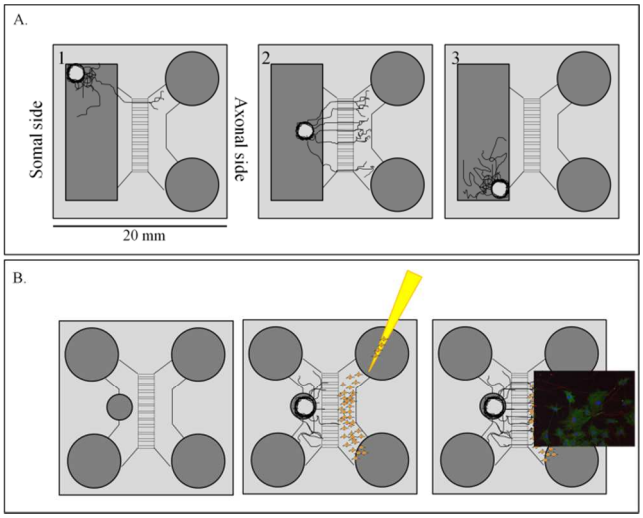

Fig.3 A. Schematic representation of the culture of entire dorsal root ganglion (DRG) in explants chambers. A. Entire adult DRG cultured in microfluidic chamber with axons crossing the microgrooves. After adhesion of DRG, MC3T3-E1 cells were seeded on axonal side. E.g. of three different possibilities (position 1, 2 and 3) for DRG's adhesion, showing that the quantity of axons that cross the microgrooves is dependent on the distance. B. Adapted microfluidic chamber for explants culture. Using original chambers as support, punch holes were performed in order to restrain the area of DRG' adhesion. Schematic representation of entire DRG from adult origin cultured in adapted microfluidic platform in coculture with MC3T3-E1 cells seeded in axonal side.

Microfluidic devices for explants culture have been described[21] nevertheless the area for DRG culture is very large related to the size of the ganglion. Therefore, the site of DRG adherence can influence the neurite density in the axonal side (Fig. 3A). In view of these evidences, the alignment of the DRG with the microgrooves axis revealed to be a crucial step in the development and optimization of the system (Fig. 3B). It was observed that, after the adjustment carried out on the somal side of the chamber, the heterogeneity of the results among different conditions and the time of DRG adhesion were significantly reduced.

Immunoreactivity to synaptic-related proteins

To further study in detail the interaction between the sensory neurons and osteoblasts *in vitro*, immunostaining against synapsin was performed. Synapsin protein has been implicated in the regulation of neurotransmitter release at synapses. It has also been showed its presence in afferent nerve endings of the skeletal muscle.[27] Using confocal microscopy we were able to obtain a 3D reconstruction of cocultures by acquiring in-focus images from selected depths. This analysis showed the presence of nerve fibers interspersed with the MC3T3-E1 cells. The neurites presented a non-uniform width and small membrane protrusions suggesting the presence of a synaptic like structures involved in the transmission of chemical signals supported by synapsin expression (Fig. 4, top).

In order to assess the maturation and function of sensory neurons in the developed coculture system, immunocitochemistry of calcitonin gene-related protein (CGRP) was performed as a marker of sensory neurons. It was observed that the neurites present in the coculture express CGRP showing that such neurites matured and were actively functional in the *in vitro* system (Fig. 4, bottom).

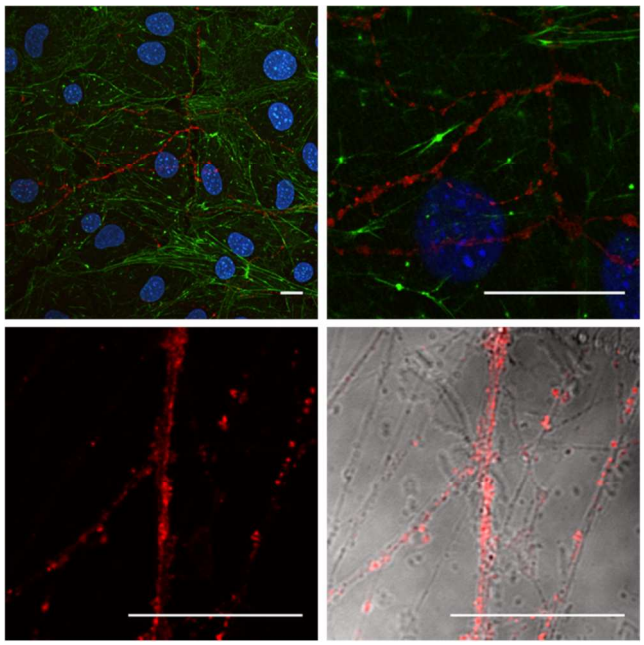

Fig.4 Immunocytochemistry against synapsin in coculture of MC3T3-E1 cells and entire DRG (top). MC3T3-E1 cells were stained in green for F-actin, neurons in red for synapsin and nuclei in blue with DAPI. Scale bar 100 µm. Immunocytochemistry against calcitonin gene-related peptide (CGRP) in coculture of MC3T3-E1 cells and entire DRG (bottom). CGRP marker of sensory neurons in red and the merged with brightfield images. Scale bar 20 µm.

Topographic and ultrastructural characterization of neurite-osteoblasts interaction

The topography of the coculture system was observed using scanning electron microscopy. MC3T3-E1 cells were identified as flattened cells showing a highly rough cytoplasm due to the presence of several organelles and proteins. They were organized as a semicontinuous layer on the surface that was traversed by the neurites extending projections (Fig. 5A). Neurites were seen as thin filaments varying size and ramifying (Fig. 5B). The neurites presented a non-uniform width suggesting the presence of varicosities associated to synaptic vesicles accumulation (Fig. 5B).

Also, growth cones were detected in the distal and leading end, forming flattened anchoring extensions to the substrate, richly equipped with filopodia (Fig. 5C). Cytoplasmic projections in the membrane of MC3T3-E1 cells were observed in contact with nerve fibers (Fig. 5D).

To achieve a high resolution characterization of the cellular ultrastructures TEM analysis was performed. MC3T3-E1 cells were easily identified by the presence of membranous organelles (mitochondria, reticulum and nucleus) and nerve fibers were distinguished by their contents of neurofilaments, microtubules and occasional groups of vesicles (Fig. 6). Transverse sections through cocultures showed neurites crossing MC3T3-E1 cells where cytoplasmic membranes can be easily identified. Tight connections (<50 nm) between cell membrane of MC3T3-E1 cells and nerve fibers were found. Moreover, highly electron density was observed in several points of the neurite membrane revealing an interaction between the two cell types (Fig. 6B).

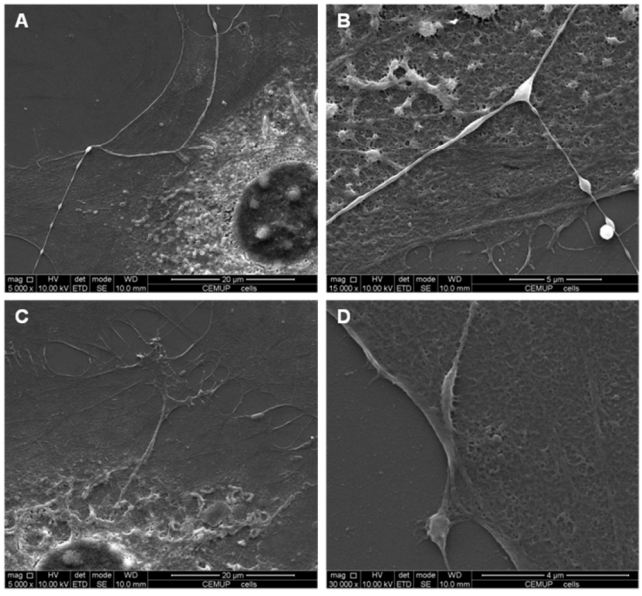

Fig.5 Images of scanning electron microscopy (SEM) of MC3T3-E1 cells and entire DRG coculture. A. Semicontinuous layer of MC3T3-E1 cells traversed by the neurites extending projections B. Thin filaments varying size and ramifying suggesting the presence of varicosities associated to synaptic vesicles accumulation. C. Growth cones in the distal and leading end, forming flattened anchoring extensions to the substrate. D. Cytoplasmic projections in the membrane of MC3T3-E1 cells were observed in contact with nerve fibers. Images acquired at 10 kV and amplifications from 1000x to 30 000x.

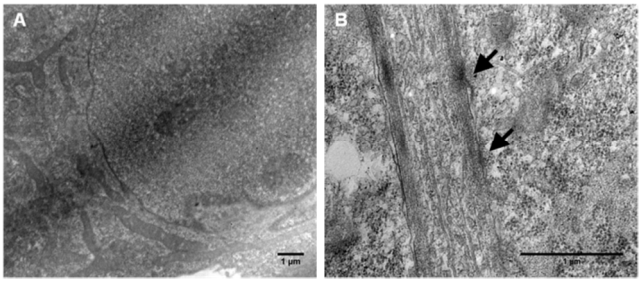

Fig.6 Images of transmission electron microscopy (TEM) of MC3T3-E1 cells and entire DRG coculture. A. MC3T3-E1 cells identified by the presence of membranous organelles (mitochondria and nucleus). B. Nerve fibers with high content of neurofilaments and microtubules. Highly electron density was observed in tight membrane connections (<50nm) (black arrows). Images acquired at 80 kV.

Mimic the extracellular matrix microenvironment

To upgrade the system, with the purpose of mimicking the properties of naturally occurring tissue extracellular matrices, which provide mechanical and biochemical signaling factors, MC3T3-E1 cells were seeded in the axonal side upon a collagen layer or within a 3D functionalized RGD-alginate matrix.

After three days of coculture, collagen coated axonal channels showed to be non-prejudicial for both MC3T3-E1 cells and DRG, the later cells projecting neurites into the axonal side. MC3T3-E1 cells showed a regular morphology. Moreover, DRG were able to extend their axons toward the coated channels where MC3T3-E1 cells were present. As shown in Fig. 7A-B, a dense axonal network was observed within the MC3T3-E1 cells.

Concerning the functionalized RGD-alginate, after three days of coculture, the MC3T3-E1 cells showed to be highly connected and spread in the matrix. Furthermore, the presence of axons within the alginate matrix in contact with MC3T3-E1 cells was detected using confocal microscopy, demonstrating their ability to grow in different substrates (Fig. 7B).

Overall, the substrates used to MC3T3-E1 cells seeding showed to be non-toxic and non-inhibitory for the axonal outgrowth. Importantly, no indicator of axonal degeneration, such as fragmentation or swelling, was detected in morphological analysis. It is noteworthy that, qualitatively, the sprouting of the nerve fibers in the collagen substrate (Fig. 7A) was more pronounced than in alginate.

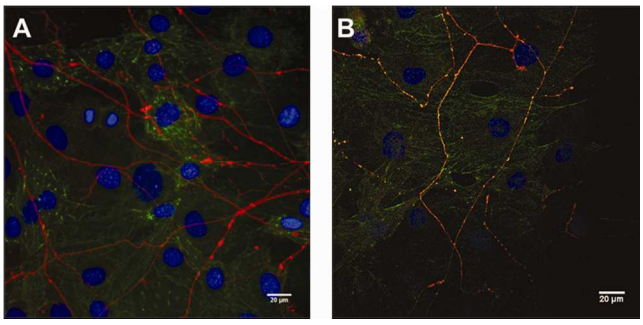

Fig. 7 Neurite network within MC3T3-E1 cells in axonal side. Representative images of MC3T3-E1 cells cocultured with entire DRG upon a collagen layer (A) or within functionalized alginate matrix (B). MC3T3-E1 cells were stained in green for F-actin, neurons in red for βIII tubulin and nuclei in blue with DAPI. Scale bar 20μm.

Computational application for quantification of axonal outgrowth

It has becoming mandatory to combine experimental readouts with computational models, in order to predict, analyze and quantify data with reproducible image analysis.[28] Quantification of the axonal growth regarding the different conditions tested was conducted. The formation of the axonal network within MC3T3-E1 cells was analyzed. DRG were stained against βIII tubulin, the actin in the cytoskeleton of MC3T3-E1 cells was marked with phalloidin and the nuclei with DAPI (Fig. 8A). For each image the spatial profile of axonal outgrowth was created. The developed program quantifies the area occupied by the neurons along the xx axis and infers about the length of the neurites in the axonal side. The three distinct domains present in the microfluidic devices (somal side-microgrooves-axonal side, Fig. 8B) can be easily distinguished in the output profile. The blue line in the profile indicates the total area of axons present in the somal side (~0-400 μm), crossing the microgrooves (~400-700 μm) and in the axonal side within MC3T3-E1 cells (~700-1500 μm). The red line indicates the unit for which the area was normalized and the green line shows the exponential fit of the degree of axonal growth within MC3T3-E1 cells (Fig. 8B).

The exponential fit is given by the spatial dependence decay function $f(x) = A \times \exp(-x/\lambda)$, where A constant returns the degree of axons that can effectively cross the microgrooves, x represents the spatial variable and the λ returns the scale of spatial decay.

Comparing the three exponential fits (Fig. 8C) it was observed that the system containing collagen and laminin showed a higher amount of axons reaching the axonal side given by the A constant (Table 1). Nevertheless, the decay spatial scale – λ – was more pronounced in these conditions than in the alginate substrate, demonstrating that axons were able to reach longer distances in the last substrate.

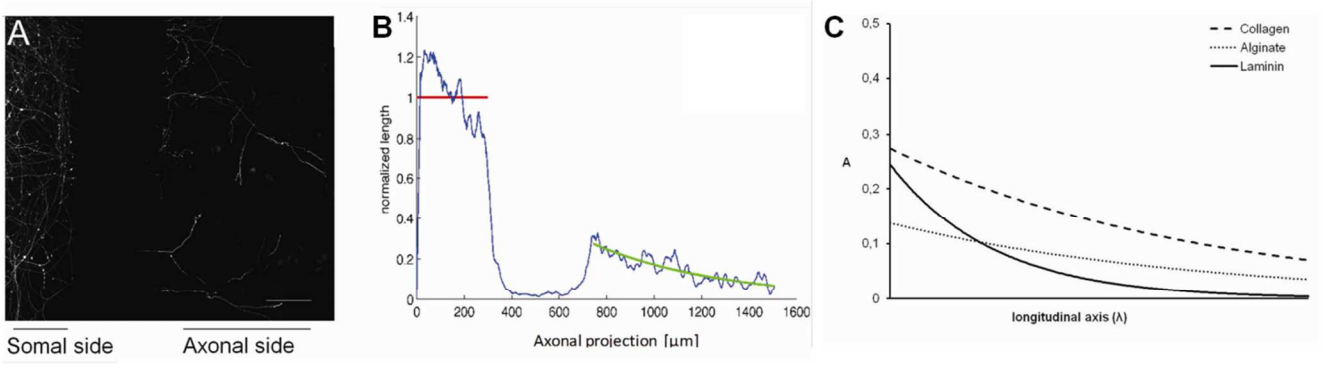

Fig 8. Output of the quantification method. Representative images used for quantification. A. Axons in white stained against βIII tubulin. Scale bar 100μm. B. Profile along the xx axis of the microfluidic device showing the area occupied by the axons (blue line), the area normalized to the somal side (red line) and the projected axons with the exponential fit (green line) in the axonal side. C. Graph representing the exponential decay function for the different substrates. In the yy axis, A value represents the quantity of axons that cross the microgrooves and reach he axonal side. Along the xx axis is represented the distance from the microgrooves.

Table 1 Values of amplitude (A) and lambda (λ) for the different substrates according to the spatial exponential decay function

$f(x) = A.e^{-x/\lambda}$	A	λ/μm
Collagen	0.27	549.7
Alginate	0.14	554.0
Laminin	0.25	184.6

[a]A value represents the quantity of axons that reach the axonal side and λ represents the distance, in μm, for which A values decreased to the half

Discussion

In this work we propose to explore the compartmentalized microfluidic devices in order to mimic the interaction between bone microenvironment and the peripheral nervous system. In fact, we were able to coculture sensory neurons and osteoblasts in distinct compartments, while preserving the ability of the nerve fibers to reach and communicate with osteoblasts, as it occurs *in vivo*.[17] The coculture system was established and characterized regarding the cell morphology, functionality, dynamic interactions and ultrastructure. Axons were detected within the osteoblasts with no observations of axonal degeneration, such as fragmentation or swelling.

Moreover, the extracellular matrix of the bone microenvironment was simulated using different substrates for the osteoblasts. Additionally, we have developed a mathematical algorithm, which enabled the automatic quantification of neurite outgrowth within microfluidic context.

The two cocultures with embryonic dissociated DRG or entire adult DRG offer different biological insights. The coculture using rat embryonic dissociated DRG and bone cells can be useful for studies of the role of peripheral nervous system in bone homeostasis during developmental stages while with entire adult DRG the coculture allow the analysis of nerve fibers and bone cells interactions in mature or challenged scenario.

Nevertheless, the coculture of entire DRG in microfluidic chambers raised a novel issue regarding the adhesion and alignment of the DRG in the somal side. The neurite outgrowth can be masked if the DRG adhere distant from the microgrooves, disabling the neurites to reach the axonal side. To surpass this issue, we have adapted the design of the normal microfluidic chamber by modifying area for DRG adhesion placing it aligned with the axis of microgrooves. This restriction allowed a faster adhesion process as well as homogeneity among the several

conditions, and improved the readout of the axonal growth.

Following the coculture assembling, the crosstalk between the nerve fibers and osteoblasts was studied in the scope of their functionality and behavior. We observed that the neurites presented small membrane protrusions immunoreactive to synapsin, implicated in the regulation of neurotransmitter release.[27] CGRP, a marker for sensory neurons, was also detected confirming the functionality of the neurites present in the *in vitro* cocultures.

Some reports have highlighted the possible direct connection between neurites and osteoblast, nevertheless the characteristics of such interaction has not been fully understood.[29, 30] SEM analysis revealed the topography of the coculture and structures as growth cones, neurite branching and the formation of varicosities where observed similar to what has been described for motor neurons.[31, 32] High-resolution characterization of the cellular ultrastructures achieved using TEM analysis showed that both sensory neurons and osteoblasts were in close contact as previously reported from *in vitro* direct contact cultures.[29, 32] Coculture models, using direct cell-cell contact, have been performed showing nerve-osteoblastic cell communication by demonstrating osteoblastic activation as a direct consequence of contact with a specific activated nerve.[14] Furthermore, under the electron microscopic observation, close membrane contacts between the neurite-like processes of DRG neurons and osteoblasts were observed. Nevertheless, the nature of this contact was not determined.[29] Herein we showed that morphological features resembling synaptic-like structures and detected by electron microscopy are supported by the presence of proteins such as synapsin and CGRP conferring functionality to the observed structures.

The nerve-osteoblasts crosstalk is strongly supported by *in vivo* studies where electron microscopy of long bones revealed the presence of nerve fibers labeling for synaptophysin, mainly localized to short nerve structures in contact to bone cells, endothelial, and bone marrow cells.[6] Moreover, ultrastructure of nerve terminals in murine bone marrow cells have also showed the presence of synaptic vesicles in the nerve fibers linked to periarterial adventitial cells.[30]

To improve the microenvironment in the microfluidic system, MC3T3-E1 cells were seeded in the axonal side upon a collagen layer or within a 3D functionalized RGD-alginate matrix.

Enrichment of hydrogels with proteins or supporting/feeder-cells was showed to improve neurite sprouting from DRG explants [33]. Collagen and functionalized alginate has been widely used for osteoblasts culture.[34, 35, 36, 37] Both in 2D or 3D these substrates have shown to be permissive also for the culture of neuronal cells allowing the neurite outgrowth.[15, 38, 39]

Our data showed that the DRG were able to project neurites towards the osteoblast lineage cultured in the axonal compartment both in 2D collagen layer or the 3D functionalized alginate matrix. Qualitative microscopic observations revealed a more pronounced axonal outgrowth and sprouting within the cells seeded upon the collagen substrate which was further confirmed by our developed quantification method.

Semi-automated or automated methods have been developed and used to assess neurite outgrowth, however these methods are mainly suitable to quantify axonal areas[40, 41] or non-suitable for dense networks.[42, 43]

To overcome these limitations, in this work we have developed an algorithm that quantifies the neurite outgrowth along the longitudinal axis in the context of microfluidic devices. Rösner *et al.*[44] have reported the quantification of axonal growth along xx axis by densiometric profile. Herein we developed an algorithm to quantify the neurite outgrowth along xx axis; however our approach relies on the area occupied by neurites after skeletonization process. By measuring the area instead of intensity we discarded the possibility of heterogeneous axonal calibers and changes in the intensity along an axon.

Our results showed differences in the spatial decay of the axonal projection. Comparing the three exponential fits, the system containing collagen and laminin substrates promoted a higher amount of axons reaching the axonal side. Nevertheless, the degree of decay was more pronounced in these conditions than in the alginate substrate revealing that axons were able to reach longer distances in the presence of alginate.

The algorithm developed demonstrated to be a powerful tool to quantify automatically, and in a non-subjective manner, the spatial extent of the neuronal network. The output is simple to interpret and researchers can easily use the program without expertise in programming. The spatial profile produces a fingerprint for the extent and properties of the axonal outgrowth (eg. may be spatially constant, decay exponentially or even produce large axonal sprouting).

Conclusions

Cocultures offer a valuable tool for validation of molecular targets identified in high throughput drug screening for bone and peripheral axonal regeneration. In the scope of bone regeneration, the optimized system proved to be advantageous for studying the cellular and molecular interactions between peripheral nervous system and bone cells.

In this work, we have applied the microfluidic devices to the coculture osteoblasts and sensory neurons with a more controlled system at the microenvironmental level. For the first time, we have performed coculture studies using entire DRG from adult origin. By electron microscopy we have detected a highly dynamic and close interaction between bone cells and sensory neurons.

Moreover the effects of different substrates, used for bone tissue engineering applications, in the axonal outgrowth were studied. The survival and outgrowth of axons projected from DRG onto different substrates demonstrated a very effective way to perform studies to understand the interaction between bone and peripheral nervous system in a context of bone regeneration strategies.

Together the entire system emerges as a potential new tool to be explored for modeling of biological processes and pharmacological screening with an automated and non-subjective tool to quantify the results.

Materials and methods

All animal experiments were conducted following approved protocols by the Ethics Committee of the Portuguese Official Authority on Animal Welfare and Experimentation (DGV).

To develop a coculture system, careful analyses of the conditions needed to ensure the viability and the maintenance of cell morphology are required. Therefore, in order to guarantee the optimal culture conditions of both cell types in the coculture system, cell morphology, viability and functionality were assessed.

1. Preparation of the microfluidic devices

The microfluidic device for neuron cell culture consisted of a molded poly(dimethlysiloxane) (PDMS) chamber placed against a glass coverslip. As described by Park *et al.*[45] the microfluidic devices were fabricated using soft lithography. Briefly, the first step comprised the fabrication of a master mold, which consists of two layers of photoresist structures on a flat silicon wafer substrate. Then, a PDMS mixture was placed over the master and incubated 3h at 37°C. Afterwards the cured PDMS molds were cut, separated from the master mold and the reservoirs were punched out followed by sterilization with ethanol 70%. The following steps were carried out in sterile conditions. Glass coverslips were coated with 0.1 mg/ml poly-D-lysine (PDL, Sigma-Aldrich), overnight at 37°C, and then washed with mQ H_2O. As soon as the glass slides were dry, the microfluidic chambers were assembled on top of the PDL coated slides. Neurobasal medium (Invitrogen) with 5 µg/ml of laminin (Sigma-Aldrich) was added to the medium reservoirs ensuring that the microgrooves connecting the compartments (somal and axonal sides – Fig. 1A) were totally filled as described in Pinto *et al.* 2012.[46]

Alignment of the entire DRG with the microgroove axis was performed. Microfluidic chambers were perforated, in the somal, using a punch key with 2 mm diameter to allow the insertion of the DRG at similar distances to the microgrooves (Fig. 3B).

2. Optimization of cell culture in axonal side

MC3T3-E1 pre-osteoblastic cell line, acquired from European Collection of Cell Cultures (ECACC, reference 99072810), were grown in alpha-minimal essential medium (α-MEM, Invitrogen) supplemented with 10% v/v heat-inactivated fetal bovine serum (FBS, Invitrogen), 10 U/ml penicillin and 10 µg/ml streptomycin (1% P/S, Invitrogen). At pre-confluence, cells were harvested using trypsin solution (0.25% w/v trypsin, 0.1% w/v glucose and 0.05% w/v ethyldiaminetetracetic acid in phosphate-buffered saline (PBS)) and were plated at different cell densities

Cell density of MC3T3-E1 cell line was tested. Cells were seeded in the axonal side at cell density of $1.5x10^4$, $1.5x10^5$ and $3x10^5$ cells/cm^2. Cells were left undisturbed for adhesion and, after 1h, α-MEM with 10% FBS was added. Monocultures performed in 96-well plates were used as controls. After three days of culture, cell morphology was observed in phase contrast microscopy (Axiovert 200, Zeiss, Germany) and metabolic activity was assessed by 3-(4,5-Dimethylthiazol-2-yl)-2,5-diphenyltetrazolium bromide (MTT) assay as described by Mosmann *et al.*[47] Briefly, 10% v/v MTT solution (Sigma-Aldrich) was added to the culture medium for 4h at 37°C. Afterwards, the formazan resulting from the reduction of MTT by mitochondrial enzymes was dissolved using dimethyl sulfoxide (Sigma-Aldrich). The amount of formazan produced was determined colorimetrically at 540 nm with normalization of interference at 690 nm, using a micro-plate spectrophotometer (Biotek Plate Reader Synergy MX).

3. Dorsal root ganglion culture in somal side

Embryonic sensory neurons were obtained from DRG of Wistar rat embryos (E14). The embryos were maintained in Hank's balanced salt solution (HBSS, Invitrogen) until DRG removal. The embryonic DRG were digested with trypsine (Sigma-Aldrich) for 15 minutes at 37°C. Digested embryonic DRG were centrifuged for 1 min at 1000 rpm to deposit the neuronal cells. Afterwards, DRG were mechanically dissociated with a flamed Pasteur pipette by pipetting up and down. Embryonic sensory neurons were plated in the somal side of the microfluidic chambers (Fig. 1A), at a density of $4x10^4$ cells/channel, previously coated with PDL and laminin [20, 45]. They were cultured with neurobasal medium supplemented with 2% v/v B-27 Serum-Free Supplement® (B-27, Invitrogen), 60µM 5-fluoro-2'-deoxyuridine (FDU, Sigma-Aldrich), 25mM glucose (Glu, Sigma-Aldrich), 1mM piruvate (Sigma-Aldrich), 50 ng/ml 7S Nerve Growth Factor (NGF, Calbiochem), 2mM glutamine (Q, BioWitacker) and 1% P/S and left undisturbed to allow adhesion.

In order to obtain organotypic cultures, entire DRG were obtained from 7-week-old C57BL/6 male mice retrieved from the excised spine and kept in HBSS. Entire DRG were plated in microfluidic chambers, coated with 0.1 mg/ml PDL and 5 µg/ml laminin, using the same culture medium as embryonic sensory neurons (one DRG/chamber – Fig. 3B). Cultures were incubated at 37°C, in humidified atmosphere with 5% CO_2 and left undisturbed until adhesion.

4. Cocultures of sensory neurons and osteoblasts

Embryonic sensory neurons were plated in the somal side of the microfluidic chambers (Fig. 1A), at a density of 4×10^4 cells/channel,[20, 45] while entire DRG were placed in the somal side of the microfluidic chamber for explants (one DRG/chamber - Fig. 3A). After adhesion, MC3T3-E1 cells were seeded in the axonal side (Fig. 3B) and the coculture was maintained during three days. Afterwards cell morphology was observed.

5. Analysis and characterization of coculture system

5.1. Immunocytochemistry

Cocultures were fixed with 2% paraformaldehyde (PFA, Merk) in tris-buffered saline (TBS) during 10 min followed by 10 min at 37ºC with 4% of PFA in TBS with 4% sucrose. Cells were permeabilized with 0.25% (v/v) Triton X-100 (Sigma-Aldrich) in TBS and incubated, for 30 min at room temperature (RT), with blocking solution composed of 5% v/v normal goat serum (Invitrogen) and 5% v/v FBS in TBS.

Neuronal cells were incubated with an antibody directed against neuronal specific marker - βIII tubulin - (Promega) diluted 1:2000, anti-calcitonin gene-related peptide (CGRP, Sigma-Aldrich) diluted 1:8000 or Synapsin (Millipore) diluted 1:1000 in blocking solution, overnight at 4ºC. Afterwards were washed and incubated 1h at RT with secondary antibody (Alexafluor 568, Invitrogen) while osteoblasts were stained with Alexa Fluor-Phalloidin 488 (Invitrogen). The glass slides were then rinsed with mQ water and mounted with Vectashield Mounting Medium with DAPI (Vector Laboratories).

Images were captured with Axiovert 200 inverted microscope equipped with AxioVision 4.8 software (Carl Zeiss, Germany) or

with confocal laser scanning microscope Leica SP2 AOBS SE equipped with LCS 2.61 software (Leica Microsystems, Germany).

5.2. Scanning electron microscopy

For scanning electron microscopic (SEM) observation, fixed cocultures were dehydrated in a graded ethanol series and critical-point dried. Samples were mounted with carbon tape and sputter-coated with gold and observed with a JEOL JSM-6301F scanning electron microscope, at 10 kV and amplifications from 1000x to 30 000x.

5.3. Transmission electron microscopy

Cocultures were fixed at 4°C for 2h with 2.5% glutaraldehyde (Merk) in 0.1 M cacodylate buffer (pH 7.2, EMS) and then with 0.15% aqueous tannic acid (Sigma-Aldrich). Samples were then post-fixed for 1h with 2% osmium tetroxide (EMS) in 0.1 M cacodylate buffer. After fixation samples were washed with distilled water, pre-stained with 1% aqueous uranyl acetate (Merk) and dehydrated in a graded ethanol series. Afterwards samples were embedded in Epon 812 resin (EMS) and let polymerize at 60ºC. Following, glass coverslip was detached with liquid nitrogen and regions of interest were selected, embedded in Epon 812 resin and polymerized for two days at 60ºC.

Ultra-thin (60–50 nm) sections were cut with an Ultramicrotome RMC PowerTome PC=XL using a diamond knife. Thin sections were collected in grids and counterstained with aqueous uranyl acetate and lead citrate (Reynolds method, Merk) before examination using a transmission electron microscope Jeol JEM 1400 (80 kV) with Orius Sc1000 Digital Camera.

6. 2D and 3D substrates in axonal side

Adapted microfluidic platforms (Fig. 3C) were used to conduct the cocultures using 2D and 3D approaches with two different substrates: collagen type I and functionalized alginate.

Entire DRG were isolated as previously described in section 3 and seeded in the somal side upon laminin coating.

MC3T3-E1 cells were seeded at 1.5 x 10^5 cells/cm^2 (corresponding to about 1.5 × 10^4 cells per microdevice) upon collagen-coated axonal side. According to manufacturer's instructions, collagen type I from rat tails (powder, Sigma-Aldrich) was dissolved in 0.1 M of acetic acid (Sigma-Aldrich). Prior to MC3T3-E1 cells seeding, a working solution of 0.01% (w/v) collagen was added to the axonal side and incubated overnight at 4°C. The remaining solution was removed and the channels were air-dried.

Functionalized alginate hydrogel was used to create a 3D microenvironment for MC3T3-E1 cells' culture. For the 3D matrix, ultra-pure alginate with high content of guluronic vs mannuronic acid units (> 60%, NovaMatrix, FMC Biopolymers) and different molecular weights were used. Low molecular weight alginate (LMW; MW<75 kDa) was used as received, whereas high molecular weight alginate (HMW; MW 75-220 kDa) was modified with the cell-adhesion peptide sequence (glycine)4-arginine-glycine-aspartic acid-serine-proline (G4RGDSP, GenScript), abbreviated as RGD. RGD was coupled to HMW alginate (16.7 mg of RGD/ml of HMW alginate) using carbodiimide chemistry, as described in detail in previous studies [48]. The alginate gel precursor solution was a 50:50 v/v binary mixture of RGD-grafted oxidized HMW (hereafter designated RGD-alginate) and LMW alginate, prepared at a final alginate concentration of 1% wt in 0.9% wt NaCl. To prepare in situ crosslinking hydrogel matrices, an internal gelation strategy adapted from Kuo *et al.* was used[49]. The alginate solution was sterile-filtered (0.22 µm) and thoroughly mixed with an aqueous suspension of $CaCO_3$ (Fluka) at a $CaCO_3$/COOH molar ratio of 1.6. To trigger gel formation, a fresh solution of glucone delta-lactone (GDL, Sigma-Aldrich) was added. The $CaCO_3$/GDL molar ratio was set at 0.125.[36, 48] The cells were homogeneously mixed at a final concentration of 1 x 10^4 cells/µl with 1% wt of alginate cell precursor and crosslinking agents as described above. Samples were placed in the incubator at 37°C under 5% CO_2 humidified atmosphere during 1h, until gelation was completed. Finally, complete medium was added to each channel.

Cocultures were maintained during three days. Afterwards, cells were stained as previously mentioned and observed using fluorescence inverted microscope. For the acquisition of the 3D cocultures images, z-stacks were acquired with laser scanning confocal microscope Leica SP2 AOBS SE equipped with LCS 2.61 software.

7. Quantification of axonal growth

Images were collected using a motorized inverted fluorescence microscope Zeiss Axiovert 200M and Micro-manager 1.3 (ImageJ) software. For the acquisition of the 3D cocultures z-stack images, laser scanning confocal microscope Leica SP2 AOBS SE was used. All analysis regarding the quantification of the axonal outgrowth was performed in MATLAB (R2010a, MathWorks, Natick, Massachusetts, U.S.A.). Images in the color channel corresponding to the neuronal marker were first preprocessed to remove background gradients through the use of morphological structuring elements (Fig. 9). The algorithm to quantify the axonal density spatial dependence uses a moving column travelling across the longitudinal axis of the image. The column has a predefined width, which balances the desired spatial resolution of the measurement with the spatial scale of heterogeneities.

Two types of analysis were performed. In the simplest analysis the algorithm works directly in the preprocessed images using the local (column) pixel intensity (reflecting neuronal marker intensity) to calculate a spatial profile of this intensity along the longitudinal axis. A second, more complex analysis was also used in which the algorithm worked on a binary mask of the axonal plexus. The binary masks were obtained using composite morphological operations in order to convert the axonal plexus into a wireframe with a single pixel diameter. Under these conditions, the total amount of non-zero pixels in a column provides a reasonable estimate of the total length of axonal fibers. The spatial profile produced in this case provides a complementary assessment in conditions where large sprouting may occur. In both types of analysis the mean amplitude of the measurement in the somal side is used for normalizing the spatial profile amplitude. This normalization provides the means to compare the transition from somal side to axonal side between different experiments.

8. Statistical analysis

Data are presented as mean ± S.E.M. (standard error of the mean). Analysis of data was performed by one-way ANOVA

followed by Dunnett's t test or Mann-Whitney U test using GraphPad Prism 5.00 for Windows (GraphPad Software, San Diego California USA). Differences between groups were considered statistically significant when *p<0.05.

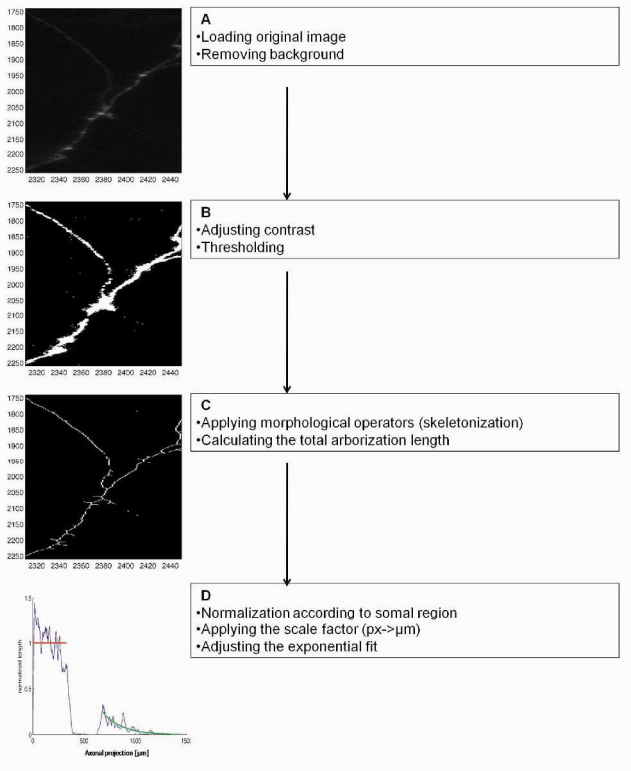

Fig.9 Processing of images with developed algorithm. A. Images are loaded as neuronal stacks. A sample image of axons stained with βIII tubulin marker is shown. B. Images are pre-processed to equalize the illumination and then a threshold is applied. C. By applying morphological operators the thresholded images are skeletonized. Skeletons are measured and normalized according to the somal region. D. Results are represented in graphic showing the area occupied by the axons (blue line), the area normalized to the somal side (red line) and the projected axons with the exponential fit (green line) in the axonal side.

Acknowledgments

This work was financed by FEDER funds through the Programa Operacional Factores de Competitividade – COMPETE and by Portuguese funds through FCT – Fundação para a Ciência e a Tecnologia in the framework of the projects PEst-C/SAU/LA0002/2011 and PTDC/SAU-OSM/101469/2008. EN and DMS are recipients of PhD fellowships SFRH/BD/81152/2011 and SFRH/BD/37654/2007, respectively. CJA and IA are recipients of Post-Doctoral fellowships SFRH/BPD/63618/2009 and SFRH/BPD/75285/2010, respectively. RDA is supported by FCT and COMPETE (PTDC/SAU-NEU/104100/2008) and by Marie Curie Actions, 7th Framework programme.

Notes and references

[a] *INEB – Instituto de Engenharia Biomédica, Rua do Campo Alegre, 823 4150-180 Porto, Portugal. *E-mail:lamghari@ineb.up.pt*
[b] *FMUP - Faculdade de Medicina da Universidade do Porto, Porto, Portugal*
[c] *IBMC – Instituto de Biologia Molecular e Celular, Universidade do Porto, Porto, Portugal*
[d] *WCU Multiscale Mechanical Design, Seoul National University, Seoul, Korea*
[e] *School of Mechanical and Aerospace Engineering, Seoul National University, Korea*
[f] *Centro de Matemática da Universidade do Porto, Porto, Portugal*
[g] *CNC – Center for Neuroscience and Cell Biology, Department of Life Sciences, University of Coimbra, Coimbra, Portugal*
[h] *ICBAS - Instituto de Ciências Biomédicas Abel Salazar, Universidade do Porto, Porto, Portugal*

1. A. C. McDonald, J. A. Schuijers, P. J. Shen, A. L. Gundlach and B. L. Grills, *Bone*, 2003, **33**. 788.
2. R. Pacifici, *Endocrinology*, 1998, **139**. 2659.
3. L. You, S. Temiyasathit, P. Lee, C. H. Kim, P. Tummala, W. Yao, W. Kingery, A. M. Malone, R. Y. Kwon and C. R. Jacobs, *Bone*, 2008, **42**. 172.
4. F. Franquinho, M. A. Liz, A. F. Nunes, E. Neto, M. Lamghari and M. M. Sousa, *FEBS J*, 2010, **277**. 3664.
5. E. L. Hill and R. Elde, *Cell and Tissue Research*, 1991, **264**. 469.
6. C. M. Serre, D. Farlay, P. D. Delmas and C. Chenu, *Bone*, 1999, **25**. 623.
7. C. Chenu, *J Musculoskelet Neuronal Interact*, 2004, **4**. 132.
8. J. Li, T. Ahmad, M. Spetea, M. Ahmed and A. Kreicbergs, *J Bone Miner Res*, 2001, **16**. 1505.
9. E. L. Hill, R. Turner and R. Elde, *Neuroscience*, 1991, **44**. 747.
10. S. E. Bove, S. J. Flatters, J. J. Inglis and P. W. Mantyh, *Brain Res Rev*, 2009, **60**. 187.
11. K. Haastert, N. Semmler, M. Wesemann, M. Rucker, N. C. Gellrich and C. Grothe, *Cell Transplant*, 2006, **15**. 733.
12. M. Zurita, J. Vaquero, S. Oya and M. Miguel, *Neuroreport*, 2005, **16**. 505.
13. K. Asada, K. Obata, K. Horiguchi and M. P. D. Takaki, *Am J Physiol Cell Physiol*, 2011.
14. K. Obata, T. Furuno, M. Nakanishi and A. Togari, *FEBS Lett*, 2007, **581**. 5917.
15. M. E. Boggs, W. R. Thompson, M. C. Farach-Carson, R. L. Duncan and T. P. Beebe, *Biointerphases*, 2011, **6**. 200.
16. H. Kamishina, J. A. Cheeseman and R. M. Clemmons, *Vet Res Commun*, 2009, **33**. 645.
17. A. Brodal, *The Somatic Afferent Pathways. In: Neurological Anatomy*. 2nd ed.; Oxford University Press: New York, 1969.
18. J. H. Yeon and J. Park, *Biochip*, 2007, **1**. 10.
19. S. Baptista, A. R. Bento, J. Gonçalves, L. Bernardino, T. Summavielle, A. Lobo, C. Fontes-Ribeiro, J. O. Malva, F. Agasse and A. P. Silva, *Neuropharmacology*, 2012, **62**. 2413.
20. A. M. Taylor, M. Blurton-Jones, S. W. Rhee, D. H. Cribbs, C. W. Cotman and N. L. Jeon, *Nat Methods*, 2005, **2**. 599.
21. J. W. Park, H. J. Kim, J. H. Byun, H. R. Ryu and N. L. Jeon, *Biotechnology Journal*, 2009, **4**. 1573.
22. I. Meyvantsson and D. J. Beebe, *Annu Rev Anal Chem (Palo Alto Calif)*, 2008, **1**. 423.
23. A. M. Taylor and N. L. Jeon, *Crit Rev Biomed Eng*, 2011, **39**. 185.
24. S. Trkov, G. Eng, R. Di Liddo, P. P. Parnigotto and G. Vunjak-Novakovic, *J Tissue Eng Regen Med*, 2010, **4**. 205.
25. Y. Gao, D. Majumdar, B. Jovanovic, C. Shaifer, P. C. Lin, A. Zijlstra, D. J. Webb and D. Li, *Biomed Microdevices*, 2011, **13**. 539.
26. D. Y. Wang, S. C. Wu, S. P. Lin, S. H. Hsiao, T. W. Chung and Y. Y. Huang, *Biomed Microdevices*, 2011, **13**. 517.
27. B. A. Petrisor, I. Ekrol and C. Court-Brown, *Foot Ankle Int*, 2006, **27**. 172.
28. I. K. Zervantonakis, C. R. Kothapalli, S. Chung, R. Sudo and R. D. Kamm, *Biomicrofluidics*, 2011, **5**. 13406.
29. K. Asada, K. Obata, K. Horiguchi and M. Takaki, *Am J Physiol Cell Physiol*, 2012, **302**. C757.
30. C. M. Court-Brown and B. Caesar, *Injury*, 2006, **37**. 691.
31. J. D. Ringe and J. J. Body, *Clin Exp Rheumatol*, 2007, **25**. 766.
32. K. Larsson, H. Brisby, B. R. Johansson, E. Runesson and B. Rydevik, *Cells Tissues Organs*, 2012, **196**. 82.

33. L. N. Novikova, A. Mosahebi, M. Wiberg, G. Terenghi, J.-O. Kellerth and L. N. Novikov, *Journal of Biomedical Materials Research Part A*, 2006, **77A**. 242.
34. R. G. LeBaron and K. A. Athanasiou, *Tissue Eng*, 2000, **6**. 85.
35. T. Braschler, R. Johann, M. Heule, L. Metref and P. Renaud, *Lab Chip*, 2005, **5**. 553.
36. S. J. Bidarra, C. C. Barrias, M. A. Barbosa, R. Soares and P. L. Granja, *Biomacromolecules*, 2010, **11**. 1956.
37. K. B. Fonseca, S. J. Bidarra, M. J. Oliveira, P. L. Granja and C. C. Barrias, *Acta Biomater*, 2011, **7**. 1674.
38. C. R. Kothapalli, E. van Veen, S. de Valence, S. Chung, I. K. Zervantonakis, F. B. Gertler and R. D. Kamm, *Lab on a Chip*, 2011, **11**. 497.
39. N. L. Francis, M. S. Shanbhag, I. Fischer and M. A. Wheatley, *J Microencapsul*, 2011, **28**. 353.
40. A. Shah, C. Fischer, C. F. Knapp and B. F. Sisken, *Journal of Neuroscience Methods*, 2004, **136**. 123.
41. J. M. Cregg, S. L. Wiseman, N. M. Pietrzak-Goetze, M. R. Smith, D. B. Jaroch, D. C. Clupper and R. J. Gilbert, *Tissue Eng Part C Methods*, 2010, **16**. 167.
42. E. Meijering, M. Jacob, J. C. Sarria, P. Steiner, H. Hirling and M. Unser, *Cytometry A*, 2004, **58**. 167.
43. M. Pool, J. Thiemann, A. Bar-Or and A. E. Fournier, *J Neurosci Methods*, 2008, **168**. 134.
44. H. Rosner and G. Vacun, *J Neurosci Methods*, 1997, **78**. 93.
45. J. W. Park, B. Vahidi, A. M. Taylor, S. W. Rhee and N. L. Jeon, *Nat Protoc*, 2006, **1**. 2128.
46. M. J. Pinto. Role of local protein synthesis in FGF22-induced presynaptic differentiation. Universidade de Coimbra, Coimbra, Portugal, 2012.
47. T. Mosmann, *J Immunol Methods*, 1983, **65**. 55.
48. M. B. Evangelista, S. X. Hsiong, R. Fernandes, P. Sampaio, H. J. Kong, C. C. Barrias, R. Salema, M. A. Barbosa, D. J. Mooney and P. L. Granja, *Biomaterials*, 2007, **28**. 3644.
49. C. K. Kuo and P. X. Ma, *Biomaterials*, 2001, **22**. 511.

